Application of 3D ERT and GPR in modern archaeology – an example for mapping new-age urban remains

Erman Lu[1*], Ercan Erkul[1], Simon L. Fischer[1], Michael Gräber[2], Wolfgang Rabbel[1]

1 Institute of Geosciences, Kiel University, Kiel, Germany
2 GeoServe – Angewandte Geophysik, Kiel
* Corresponding author: E-mail: stu219656@mail.uni-kiel.de

Abstract
The aim of this study is to find out to what extent 3D geoelectric surface measurements can contribute better to a high-resolution subsurface model than conventional 2D measurements. 2D and 3D electrical measurements as well as GPR measurements were performed on a former working farm in Kiel. The results of the 3D electrical measurements show that individual structures in the subsurface can be detected better than in the results of the 2D electrical measurements. These structures are also visible in the GPR time slices.

Keywords
DC resistivity; GPR; urban archaeological prospection; 3D ERT; 3D inversion

Introduction

In engineering geophysics, 2D geoelectrical measurements are often used. 2D measurements assume a subsurface model which is as constant as possible perpendicular to the section plane of a profile. Hereby it must be considered that unknown 3D structures lead to distortion of the calculated subsurface model (Yang and Lagmanson 2006). In this study, 2D and 3D measurements were conducted on an urban test area (25 m x 25 m) in Kiel (Fig. 1) using the RESECS multi-channel measurement system by GeoServe (geoserve.de 2023). The aim of this study is to find out how far the 3D geoelectric surface measurements can contribute to a high-resolution subsurface model better than conventional 2D measurements. In addition, the high-resolution ground penetrating radar (GPR) measurements are used for the independent acquisition of the 3D structures. The results of the 2D and 3D inversions were compared and combined with the GPR results.

Methods

In this study 3D ERT data were acquired using a RESECS (PC controlled DC resistivity meter system) by GeoServe. Eight parallel survey lines and a total of 206 electrodes were used to set up an 8 m by 25 m rectangular survey grid (Fig. 2). The in-line and cross-line separations were 1 meter. By moving the survey grid, the square survey area was covered. Pole-pole and dipole-dipole configurations were measured. The data was processed with the open-source inversion program BERT (resistivity.net 2018) and the commercial programs Res2DInv, Res3DInv. ground penetrating radar (GPR) measurements were conducted with a GSSI dual-frequency antenna (300 MHz and 800 MHz), which was mounted on a four-wheel cart. A differential GPS by STONEX was used for positioning of the system. The results of the 3D ERT inversions were compared and combined with the GPR results.

Results and discussion

Four anomalies are observed in the 3D ERT depth slice at 0.5 m (Fig. 3). Anomaly A has a rectangular shape with high resistivity. Within this rectangular structure, the resistivity is lower than the background. Southwest of anomaly A is anomaly B. Its rectangular shape and high electrical

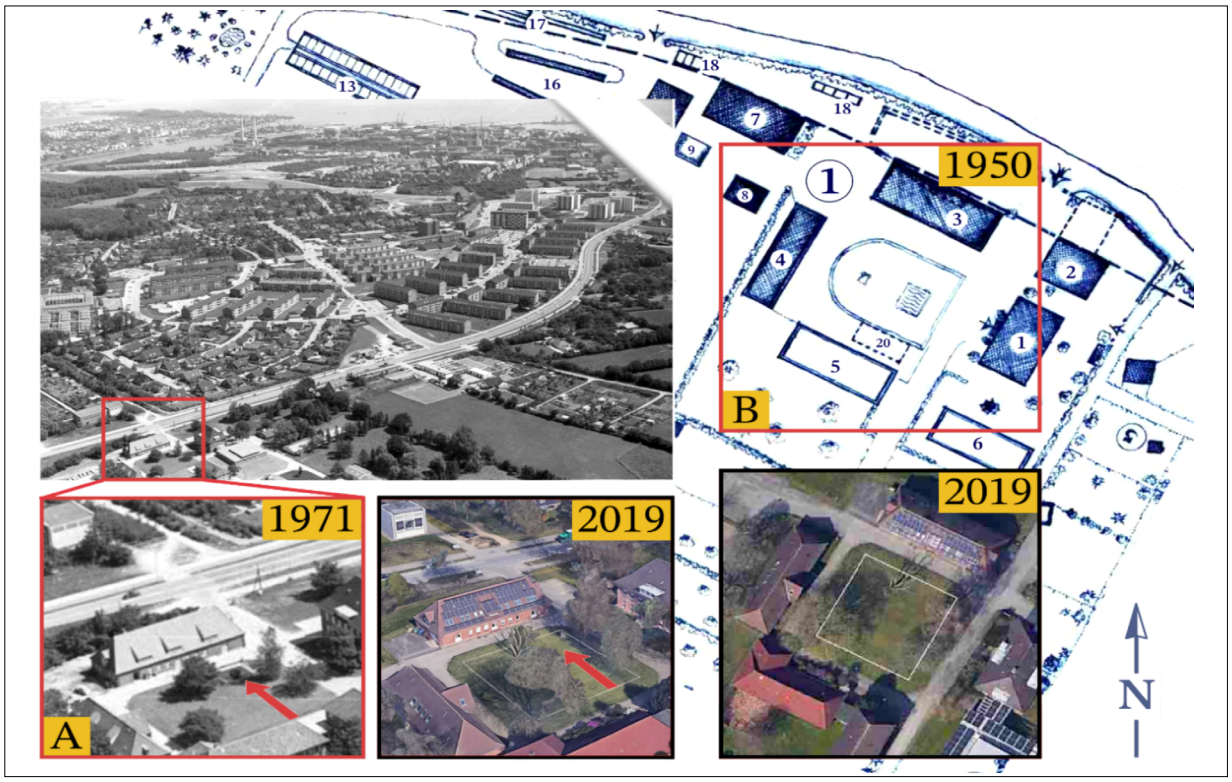

Fig. 1: a) The aerial photograph shows the survey area in 1971 (fotoarchiv-stadtarchiv.kiel.de 2023 , Sig. 49.261, CC BY-3.0 SA DE). The red arrow shows a rectangular structure that no longer exists. b) The survey area (base map: Google, ©2023 AeroWest, CNES/Airbus, GeoBasis-DE/BKG, Maxar Technologies, ©2023 GeoBasis-DE/BKG (© 2009)) had been a working farm in 1950, a U-shaped lawn with a smaller surface area than today's. On the U-shaped lawn was drawn a rectangular structure with waves symbol. The old basement (building number 20 on the yard plan, drawn with dashed line) was located outside the U-shaped lawn, but should be within the southern area of the survey area.

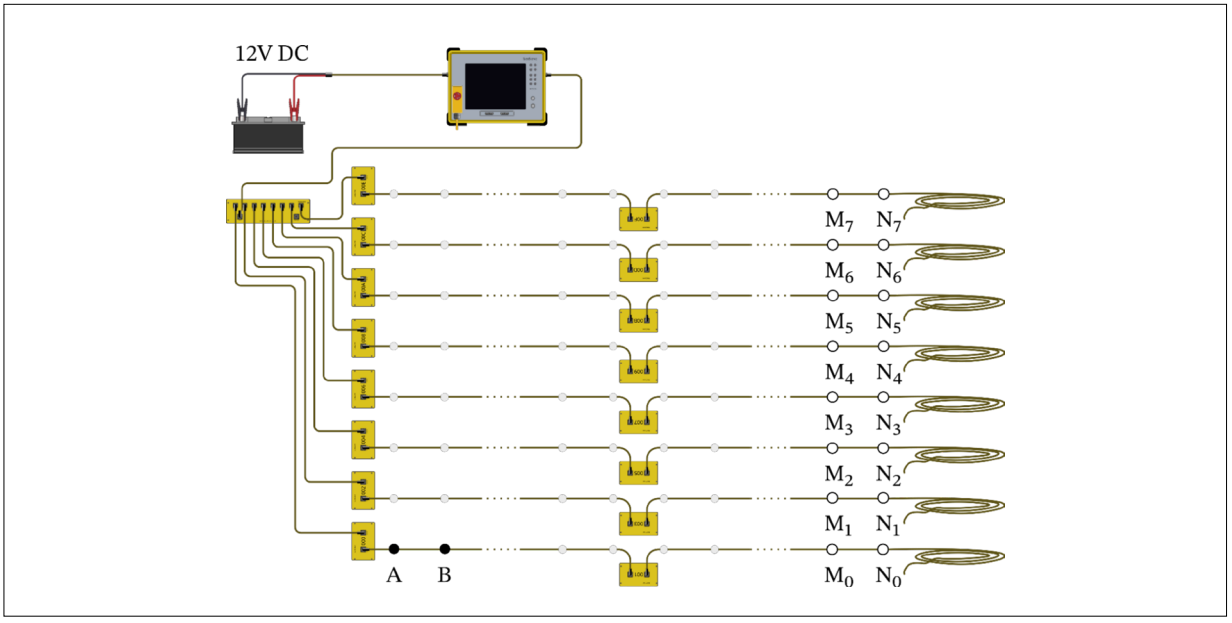

Fig. 2: Measurement setup for 3D ERT. A, B (in black) as current electrodes and M0 to M7, N0 to N7 (in white) as potential electrodes. The electrodes form a rectangular grid. The grid spacing is 1 m.

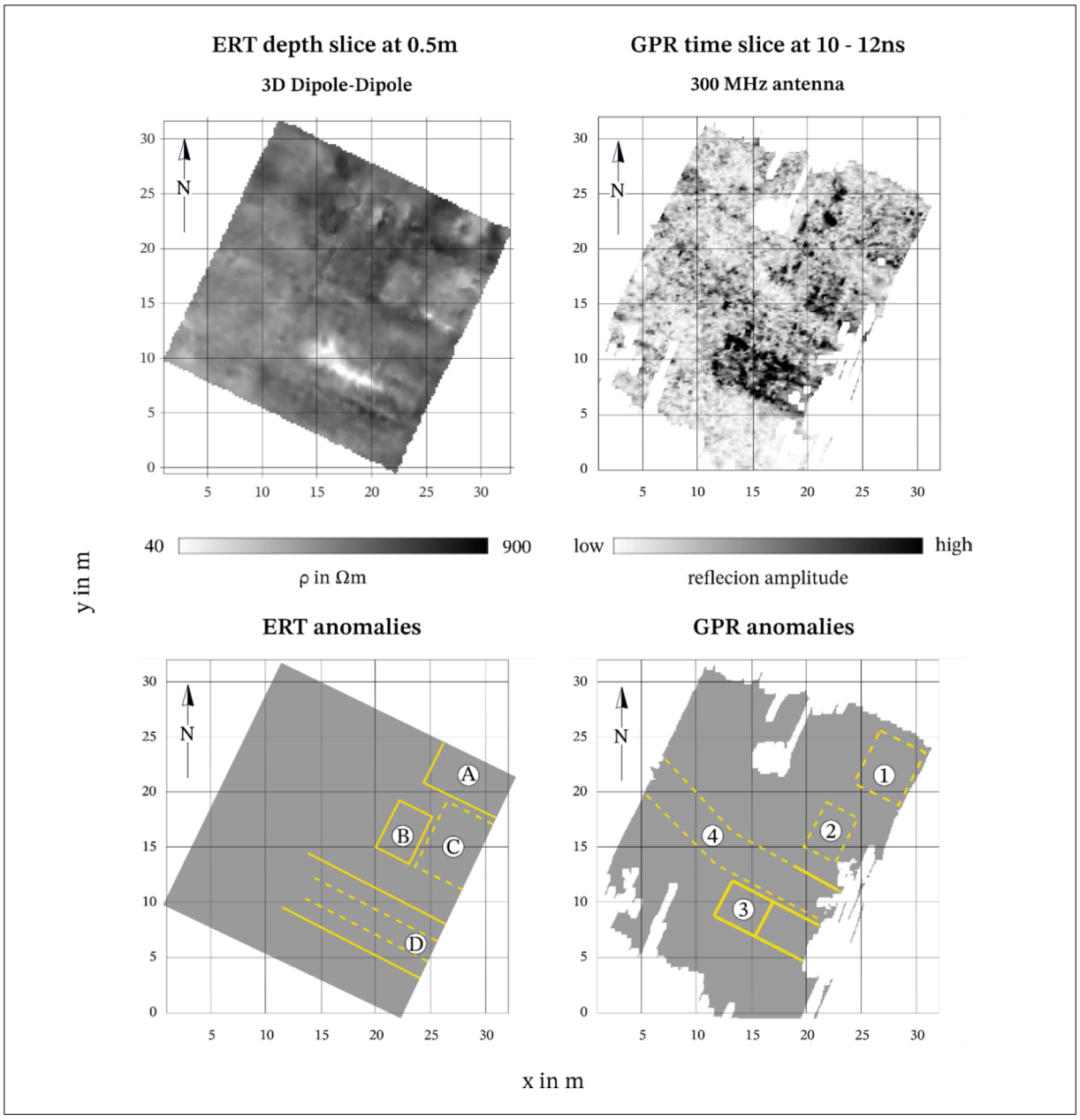

Fig. 3: Comparison of GPR and 3D ERT results. By evaluating the diffraction hyperbolas, an average radar wave propagation speed of 8 cm/ns was determined. 10 – 12 ns is equivalent to a depth of approx. 0.4 - 0.5 m. The two-dimensional patterns are marked with dashed lines. The linear structures are marked with solid lines.

resistivity stand out from the background. On the western side of anomaly B a rectangular area is characterized by low resistivity values (anomaly C, marked with dashed lines). Parallel linear structures are observed in area D. A region of low resistivity values can be observed between the dashed linear structures. The position of anomaly A in the depth slice correlates well with that of anomaly 1 in the GPR time slice. These anomalies could be caused by the remains of the rectangular structure in the northeast corner of the survey area (Fig. 1). anomalies B and 2 have approximately the same size and orientation. The position of the old basement, drawn with dashed lines on the yard plan (Fig. 1), coincides with anomaly 3 in the GPR time slice and anomaly D in the ERT depth slice. It is assumed that these anomalies are caused by the old basement. The low resistivity area within anomaly D can be interpreted as the

possibility that the fill or fill material within the basement is not consolidated and the water content within could be higher than the surrounding area. In the ERT depth slices at 0.9 m, the anomalies are still visible in the 3D inversion result, while they are poorly visible in the 2D inversion result. In the depth-resistivity section, the 2D and 3D inversion results show a similar distribution of the resistivity, but the 3D inversion result is more detailed and the transitions between high and low resistivity regions are more contrasting.

Conclusion

The results of the 3D measurements show that both in the electrical depth sections and in the depth-resistivity sections up to a depth of 1.5 m individual structures can be detected better than in the results of the 2D measurements. These structures can also be confirmed by the results of GPR. The linear and rectangular anomalies mapped in the depth slices of the 3D ERT inversion are seen in the GPR time slices to the corresponding depth.

References

fotoarchiv-stadtarchiv.kiel.de [Internet]. Luftaufnahme Projensdorf; c2023 [cited 2023 Jan 27]. Available from: https://fotoarchiv-stadtarchiv.kiel.de/zvimg.FAU?sid=ACCE8EB3&dm=1&qpos=49758&erg=A &ipos=1&=fotos.jpg&hst=1

geoserve.de [Internet]. GeoServe angewandte Geophysik; c2023 [cited 2023 Jan 6]. Available from: https://www.geoserve.de/index.php

resistivity.net [Internet]. Boundless Electrical Resistivity Tomography BERT - the user tutorial; c2018 [cited 2022 Sep 1]. Available from: http://www.resistivity.net/download/bert-tutorial.pdf

Yang X, Lagmanson M. Comparison of 2D and 3D Electrical Resistivity Imaging Methods. Proceeding of 19th Symposium on the Application of Geophysics to Engineering and Environmental Problems (SAGEEP 2006); 2006 Apr 2-6; Seattle, Washington, USA. Denver: Environmental and Engineering Geophysical Society (EEGS); 2006. p. 585-594. doi: 10.4133/1.2923695

Open Access

This paper is published under the Creative Commons Attribution 4.0 International license (https://creativecommons.org/licenses/by/4.0/deed.en). Please note that individual, appropriately marked parts of the paper may be excluded from the license mentioned or may be subject to other copyright conditions. If such third party material is not under the Creative Commons license, any copying, editing or public reproduction is only permitted with the prior consent of the respective copyright owner or on the basis of relevant legal authorization regulations.